

# On the coupling between helium settling and rotation-induced mixing in stellar radiative zones : II- Numerical approach

Sylvie Théado and Sylvie Vauclair

*Laboratoire d'Astrophysique, Observatoire Midi-Pyrénées, 14 avenue Edouard Belin, 31400  
Toulouse, France*

## ABSTRACT

In the first paper of this series, we discussed analytically, in an approximate way, the mixing processes which occur in slowly rotating stars when the feed-back effects due to the diffusion-induced  $\mu$ -gradients are introduced in the computations. We found that the classical scheme of meridional circulation was dramatically modified, with important possible consequences. Here we present a complete 2D numerical simulation of these processes in a static stellar model. The helium microscopic diffusion and the meridional advection are computed simultaneously, so that we can follow the evolution of the abundances and mixing processes in the radiative zone. Most of the effects discussed in paper I are confirmed. Some consequences will be discussed in a forthcoming paper (Théado and Vauclair 2002, paper III).

*Subject headings:* stars: abundances; stars: rotation-induced mixing; diffusion ;  
2D numerical simulation

## 1. Introduction

This paper is the second of a series concerning the importance of diffusion-induced  $\mu$ -gradients in the computations of rotation-induced mixing in stellar radiative zones. In the first paper of this series (Vauclair and Théado 2002, paper I), we discussed in details the orders of magnitude of the various terms which appear in the computation of the meridional circulation velocity. We showed that the term related to the transport of angular momentum may be important in some cases and particularly at the beginning of the main-sequence for F and G type stars. However, during most of their lifetime, their hydrodynamical history is

dominated by the competition between the classical terms (the Eddington-Sweet meridional circulation) and the terms related to the feed-back effect induced by  $\mu$ -gradients.

The situation which appears when these terms become of the same order of magnitude and nearly cancel out is difficult to handle numerically. In paper I we gave an approximate analytical approach to better understand, in a physical way, the hydrodynamical processes which may happen when this situation takes place. We found that a quasi-stationary stage can settle down, in which case the circulation pattern is strongly modified. The vertical and horizontal  $\mu$ -gradients adjust themselves to remain nearly constant in the concerned zone. Such a situation must be taken into account in the computations of abundance variations in stellar outer layers.

In the past, various authors performed 2D numerical simulation of meridional circulation (Tassoul and Tassoul (1982), Mestel and Moss (1986), Charbonneau (1992)). In the computations of Tassoul and Tassoul (1982) and Mestel and Moss (1986) the importance of the feed-back effect due to nuclearly-induced  $\mu$ -gradients was recognized. In particular Mestel and Moss (1986) showed that the  $\mu$ -currents could slowly stabilize the circulation near the core. They called this process “creeping paralysis”. However in these computations the feed-back effect due to the diffusion-induced  $\mu$ -gradients was not included and the horizontal and vertical composition variations induced by the diffusion/circulation coupling were not accurately studied.

In this paper, we present the results of a 2D numerical simulation of meridional circulation in the presence of helium settling, including the feed-back effect due to  $\mu$ -gradients. In order to calculate and visualize in a realistic way the physical processes which take place below the convective zone, we have computed simultaneously the helium abundance variations and the meridional circulation velocity. No free parameter is introduced in these computations, although some simplifying assumptions are made : the rotation velocity is assumed constant during the time of the simulation, and the modifications of the stellar structure induced by diffusion and evolution are neglected (static model). In the simulation, the meridional circulation is treated as an advection process. However, as will be discussed in section 2.2, the discretization leads to some numerical diffusion, which we evaluate and find similar to an anisotropic mixing, larger horizontally than vertically, in a realistic way.

In section 2 we give a complete description of the numerical method. The simulation is first tested on the well-known classical circulation (section 3) and the results obtained including the effects of  $\mu$ -gradients are given in section 4. A general discussion of these results is proposed in section 5.

## 2. Numerical analysis

We describe below the details of our computational method. Throughout this paper, we use the spherical coordinate system but we assume axial symmetry so that the studied processes are reduced to a 2D simulation.

### 2.1. Discretization

As an initial model for our simulation, we used a standard homogeneous stellar model (here we chose a  $0.75M_{\odot}$  halo star, which has no importance for the general process we intent to describe). To obtain the 2D meshpoint of the simulation, each shell of the 1D initial model is first discretized in the latitudinal direction into angular sectors of one arcdeg (figure 1).

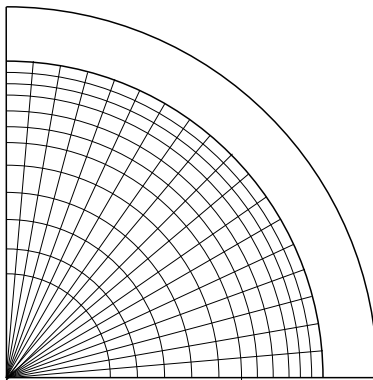


Fig. 1.— Discretization of a meridional plane quadrant (schematic representation). In the computations the model is divided in about 800 shells in the vertical direction and 90 angular sectors in the horizontal direction. The meshpoint is tighter in the vertical than in the horizontal direction.

In order to treat in a more accurate way the advection by meridional circulation and to reduce the numerical diffusion, a secondary meshpoint will be defined : each cell of the main meshpoint will be divided into smaller cells. We will come back on this secondary meshpoint in section 2.2.2.

### 2.2. Computational method

This simulation aims to understand the coupling between microscopic diffusion and meridional circulation. These two physical processes have quite different natures and be-

haviors. Microscopic diffusion is a particle process which leads to a selective transport of chemical elements. On the other hand, meridional circulation is a hydrodynamical process which leads to a global transport of matter. We have included in the code two different routines which compute each of the two transport processes in an adequate way :

- a particle routine which first computes the microscopic diffusion of helium with an eulerian scheme,
- a hydrodynamical routine which includes a lagrangian description of the transport process to compute the global advection by meridional circulation.

At each timestep, we first compute the diffusion-induced composition variations by using the particle routine. Then, taking into account the new chemical composition, we determine the circulation-induced abundance variations by computing the advection of matter with the hydrodynamical routine.

The timesteps always satisfy the flow condition. Using smaller timesteps does not alter the results. We have also checked that reversing the order of the diffusion and circulation computations does not alter the results in a significant way.

### 2.2.1. *The treatment of microscopic diffusion*

The diffusion-induced composition variations are computed by solving the helium mass conservation equation:

$$\frac{\partial \rho Y}{\partial t} + \text{div}(\rho \mathbf{V} Y) = 0 \quad (1)$$

where  $Y$  represents the helium mass fraction and  $\mathbf{V}$  the helium diffusion velocity. In the region below the convective zone, the helium production rate by nuclear reactions is negligible.

The diffusion velocity is computed in the test-atom approximation with respect to hydrogen :

$$\mathbf{V} = D_{He} \left\{ -\nabla \ln c_{He} + k_p \nabla \ln p + k_T \nabla \ln T + \frac{m \mathbf{F}}{kT} \right\} \quad (2)$$

$D_{He}$  is the helium diffusion coefficient in a hydrogen gas, which we compute with the Paquette et al. (1986) formalism, and the four terms in the bracket represent respectively the concentration gradient, the gravitational settling, the thermal and the radiative diffusion.

The test-atom approximation is rather crude for helium, whose abundance is about 10% that of hydrogen. However, for the purpose of the present paper, treating helium diffusion

with a more precise approximation would have lead to useless heavier computations in the 2D simulation with a difference in the results of 10 to 15 % (Montmerle and Michaud (1976)).

In solar type stars, the radiative acceleration is negligible. In the vertical direction, the diffusion velocity is then due to the concentration gradient, the gravitational settling and the thermal diffusion. In the horizontal direction the velocity depends only on the concentration gradient.

The horizontal and the vertical component of  $\nabla \ln c_{He}$  are respectively equal to :  $\frac{1}{r} \frac{1}{c} \frac{\partial c}{\partial \theta}$  and  $\frac{1}{c} \frac{\partial c}{\partial r}$ . As a first approximation, the helium concentration is a linear function of the inverse of the molecular weight so  $\frac{dc}{c}$  can be approximated by  $\frac{d\mu}{\mu}$ .

In the horizontal direction, we will see in section 4 that in the considered stars  $\frac{d\mu}{\mu}$  is typically of the order of  $10^{-6}$ . With a radius of about  $5 \cdot 10^{10}$  cm, it leads to the following approximation :

$$\left| \frac{1}{r} \frac{1}{\mu} \frac{\partial \mu}{\partial \theta} \right| \simeq 2 \cdot 10^{-17} \text{cm}^{-1}$$

This leads to a horizontal diffusion velocity of nearly  $8 \cdot 10^{-17}$  cm.s<sup>-1</sup> while the horizontal meridional velocity is typically of the order of  $10^{-8}$  to  $10^{-9}$  cm.s<sup>-1</sup> : the horizontal diffusion can therefore be neglected in the computations.

In the vertical direction  $\left| \frac{1}{c} \frac{\partial c}{\partial r} \right|$  can be approximated by  $\left| \frac{1}{\mu} \frac{\partial \mu}{\partial r} \right|$ . We will see in section 3.1 that just below the convective zone, where the  $\mu$ -gradients are the steepest :

$$\left| \frac{1}{\mu} \frac{d\mu}{dr} \right| \simeq 9 \cdot 10^{-12} \text{cm}^{-1}$$

It is interesting to compare the concentration gradient contribution with the others terms and in particular the gravitational settling term. In the case of a totally ionised gas, this term can be written :

$$k_p \nabla \ln p = \frac{5 m_p}{2 k T} \frac{G m_r}{r^2}$$

In a  $0.75 M_{\odot}$  (i.e. a radius of nearly  $5 \cdot 10^{10}$  cm), this term is approximately  $1.7 \cdot 10^{-9}$  cm.s<sup>-1</sup>. Typically the vertical concentration gradient term is at least 2 order of magnitude smaller than the other terms.

Two boundary conditions are needed. The upper one is obtained by computing the dilution in the convective zone.

$$\int_{cz} \frac{\partial \rho X}{\partial t} dv + \int_{cz} \rho X \mathbf{V} \cdot d\mathbf{S} = 0 \quad (3)$$

which can be written in quasi-stationary regime :

$$M_c \frac{\partial X}{\partial t} = 2\pi \int_0^\pi \rho X V_r r^2 \sin \theta d\theta \quad (4)$$

where  $M_c$  is the stellar convective mass.

The nuclear reaction rates are neglected and we assume that the diffusion time scale is much greater than the stellar life : in these conditions, the lower boundary condition is chosen so that  $Y = \text{constant}$  below  $r \simeq 0.4 R_\odot$ .

### 2.2.2. The treatment of meridional circulation

The vertical component of the meridional circulation is traditionally expanded in spherical functions. When the rotation rate depends only on depth, the radial velocity involves only the second Legendre polynomial :

$$u_r = U_r P_2(\cos \theta) \quad (5)$$

The velocity amplitude,  $U_r$ , is derived from the heat transfert equation. It can be written (Vauclair and Théado 2002, paper I):

$$U_r = \frac{P}{\rho g T C_p (\nabla_{ad} - \nabla + \nabla_\mu)} \frac{L}{M_*} (E_\Omega + E_\mu + E_\zeta + E_h) \quad (6)$$

$\nabla_{ad}$  and  $\nabla$  represent the usual adiabatic and real ratios  $\left(\frac{d \ln T}{d \ln P}\right)$ ,  $\nabla_\mu$  the mean molecular weight contribution  $\left(\frac{d \ln \mu}{d \ln P}\right)$ . The four terms in the bracket represent :

- the classical Eddington-Sweet term  $E_\Omega$  :

$$E_\Omega = 2 \left[ 1 - \frac{\bar{\Omega}^2}{2\pi G \bar{\rho}} \right] \frac{\tilde{g}}{\bar{g}} - \frac{\rho_m}{\bar{\rho}} \left\{ \frac{r}{3} \frac{d}{dr} \left[ H_T \frac{d\zeta}{dr} - \chi_T \zeta \right] - \frac{2H_T}{r} \zeta + \frac{2}{3} \zeta \right\} - \frac{\bar{\Omega}^2}{2\pi G \bar{\rho}} \zeta \quad (7)$$

Note that the last term in this equation was not written in the previous papers : it was neglected by mistake in Maeder and Zahn 1998. While it is indeed negligible in the deep stellar regions where the so-called “Gratton-Öpik term” is less than unity, it can become important in the outer layers.

- the  $\mu$ -gradient term  $E_\mu$  :

$$E_\mu = \frac{\rho_m}{\bar{\rho}} \left\{ \frac{r}{3} \frac{d}{dr} \left[ H_T \frac{d\Lambda}{dr} - (\chi_\mu + \chi_T + 1) \Lambda \right] - 2 \frac{H_T}{r} \Lambda \right\} \quad (8)$$

- the term related to the differential rotation  $E_\zeta$  :

$$E_\zeta = \frac{M_*}{L} \bar{T} C_p \frac{\partial \zeta}{\partial t} \quad (9)$$

- the term related to horizontal turbulence  $E_h$  :

$$E_h = \frac{\rho_m}{\bar{\rho}} \frac{2H_T}{r} \frac{D_h}{K} \zeta \quad (10)$$

In these equations,  $\zeta$  represents the density fluctuations along a level surface  $\frac{\tilde{\rho}}{\bar{\rho}}$  ;  $\Lambda$  refers to the horizontal  $\mu$ -fluctuations  $\frac{\tilde{\mu}}{\bar{\mu}}$  ;  $\rho_m$  is the mean density inside the sphere of radius  $r$  while  $\bar{\rho}$  represents the density average on the level surface (as well as  $\bar{T}$  for the temperature and  $\bar{\Omega}$  for the angular rotation velocity) ;  $C_p$  is the specific heat ;  $H_T$  the temperature scale height and  $D_h$  the horizontal turbulent diffusion coefficient.  $\chi_\mu$  and  $\chi_T$  are given by :

$$\chi_\mu = \left( \frac{\partial \ln \chi}{\partial \ln \mu} \right)_{P,T} \quad ; \quad \chi_T = \left( \frac{\partial \ln \chi}{\partial \ln T} \right)_{P,\mu}$$

In paper I, we showed that the term  $E_h$  due to horizontal turbulence is always negligible compared to the other terms. We also showed that the term  $E_\zeta$ , which is related to the transport of angular momentum, may be important at the beginning of the stellar lifetime. We neglect it here however, as our purpose is to study the behavior of the circulation when the two other terms  $E_\Omega$  and  $E_\mu$  are preponderant.

The horizontal velocity component of the meridional circulation is then deduced from the equation of matter conservation:

$$\text{div}(u_r \rho r^2) = -u_\theta \rho r \quad (11)$$

which gives :

$$u_\theta = -\frac{1}{2\rho r} \frac{d}{dr} (\rho r^2 U_r) \sin \theta \cos \theta \quad (12)$$

### 2.2.3. The numerical method

We use the finite difference technique to discretize the equations. The timestep of the simulation is computed in order to satisfy the flow condition. At each timestep, the microscopic diffusion is first computed by determining the helium diffusion velocity in each

shell and solving the helium mass conservation equation for each cell of the meshpoint. Once the diffusion-induced abundance variations are computed in the whole star, the laminar meridional circulation is then treated as an advection process. The velocity components are first determined at the center of each cell. Then, in order to treat in a more accurate way the advection by circulation and to reduce the numerical diffusion, a secondary meshpoint is introduced in the computations. Each cell of the main meshpoint (described in figure 1) is discretized into  $10^4$  smaller cells. All the secondary cells belonging to the same main cell are supposed to be advected with the same velocity : the one computed at the center of the main cell. This assumption introduced an error lower than 5% on the velocity components. The matter contained in each cell of the secondary meshpoint is supposed to be concentrated at its center. The motion of each secondary cell is computed and the contained matter is distributed into the main cell in an adequate way (see figure 2). The main cells are then homogenized to obtain the new chemical composition in the star.

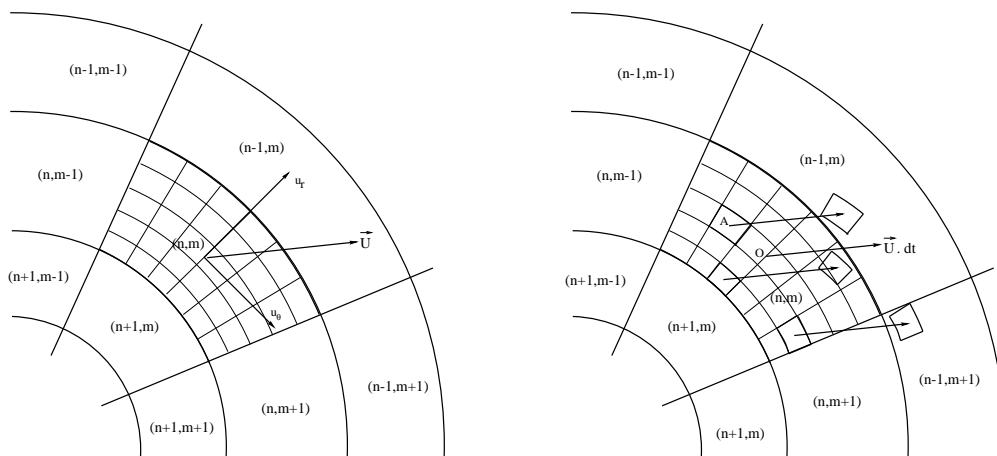


Fig. 2.— Schematic representation of the meridional circulation advection : secondary meshpoint and cell advection.

### 2.3. Numerical diffusion

In spite of the secondary meshpoint introduced in the computations of meridional circulation, the numerical scheme suffers some numerical diffusion. This is basically due to the fact that, at each time step, matter is homogenized inside each cell of the main meshpoint.

The numerical diffusion cannot be totally suppressed, however it can be reduced by increasing the number of cells. In practice increasing the number of cells leads rapidly to

extremely large computations time which are unacceptable. The  $800 \times 90$  chosen meshpoint leads to both reasonable computation times and reasonable numerical diffusion.

It is possible to evaluate this diffusion by defining an anisotropic numerical diffusion coefficient which we call  $D_h^{num}$  in the horizontal direction and  $D_v^{num}$  in the vertical direction. In both case it is defined as  $D^{num} = dr^2/dt$  where  $dr$  is the length scale of the cell and  $dt$  the time step of the computation.

In the horizontal direction  $dr \simeq r/100$  while in the vertical one  $dr \simeq r/1000$ . The time steps of the simulation lie between  $10^6$  and  $10^7$  yr. With a radius of about  $5 \cdot 10^{10}$  cm, we find the orders of magnitude :  $D_h^{num} \simeq 10^3$  to  $10^4$   $\text{cm}^2 \cdot \text{s}^{-1}$  and  $D_v^{num} \simeq 10$  to  $100$   $\text{cm}^2 \cdot \text{s}^{-1}$ .

It is interesting to compare the value of the numerical horizontal diffusion coefficient with the prescription given by Zahn (1992) and Maeder and Zahn (1998):  $D_h = C_h r \cdot U_r$ . With  $U_r$  of order  $10^{-7}$   $\text{cm} \cdot \text{s}^{-1}$ , we find  $C_h \simeq 0.2$  to  $2$ , which is quite reasonable. Meanwhile the numerical vertical diffusion coefficient is 100 times smaller.

We thus find that our numerical scheme leads to some small artificial mixing, which simulates in a realistic way the kind of turbulence which may occur physically in such a situation.

### 3. Test of the numerical scheme

To test the numerical scheme, we first check that the simulation reproduces correctly the processes we already know, like microscopic diffusion alone and classical meridional circulation, without the  $\mu$ -terms. Then we introduce the feed-back effect due to the  $\mu$ -gradients to try to understand more precisely what happens in those circumstances.

#### 3.1. The classical meridional circulation

We first introduce in the simulation the diffusion of helium and the advection by the  $\Omega$ -currents only : the effects of  $\mu$ -gradients are not taken into account, which means that the  $E_\mu$  term is not introduced in the computations of the meridional velocity.

Here we present the results obtained for a constant rotation velocity of  $5 \text{ km} \cdot \text{s}^{-1}$ . The circulation streamlines are represented on figure 3. As expected, the circulation leads to ascending flows near the rotation axis and to descending flows near the equator. The flow brings  $\mu$ -enriched matter up in the polar axis and  $\mu$ -depleted matter down in the equatorial regions. Figure 4 displays the molecular weight profiles at different steps of the simulation.

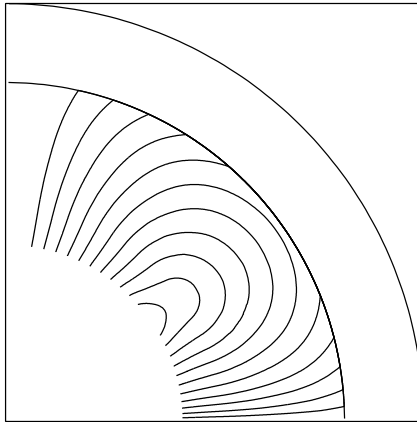


Fig. 3.— Meridional circulation streamlines : here, only the  $\Omega$ -currents are taken into account in the meridional velocity computations. The rotation velocity is chosen constant during the whole simulation and no structural evolutions are introduced in the computations, therefore the  $\Omega$ -currents streamlines remain the same at each timestep.

For comparison it also shows the results obtained when helium diffusion is the only transport process introduced in the computations (i.e. without meridional circulation). Microscopic diffusion alone leads to an important vertical  $\mu$ -gradient below the convective zone. The spread of the molecular weight values obtained in the presence of meridional circulation shows how  $\Omega$ -currents turn the diffusion-induced vertical  $\mu$ -gradients into horizontal ones.

### 3.2. Importance of $\mu$ -currents

In the previous section we have presented the molecular weight variations under the combined effects of helium diffusion and  $\Omega$ -currents only. We have shown that diffusion builds vertical  $\mu$ -gradients which are turned into horizontal ones by  $\Omega$ -currents. Although the  $\mu$ -currents are not taken into account in the computations of meridional advection, we have computed at each time step the value of the  $E_\mu$  term by determining the horizontal  $\mu$ -gradients built in the star and using equation 8. We insist on the fact that these  $\mu$ -gradients are those built by the classical meridional circulation, i.e. when the feed-back effect of  $\mu$ -currents is not taken into account.

In these conditions, figure 5 (left column) displays the molecular weight versus the colatitude at different depths below the convective zone and at different steps of the computations. This shows the slow construction of the horizontal  $\mu$ -currents. Figure 5 (right

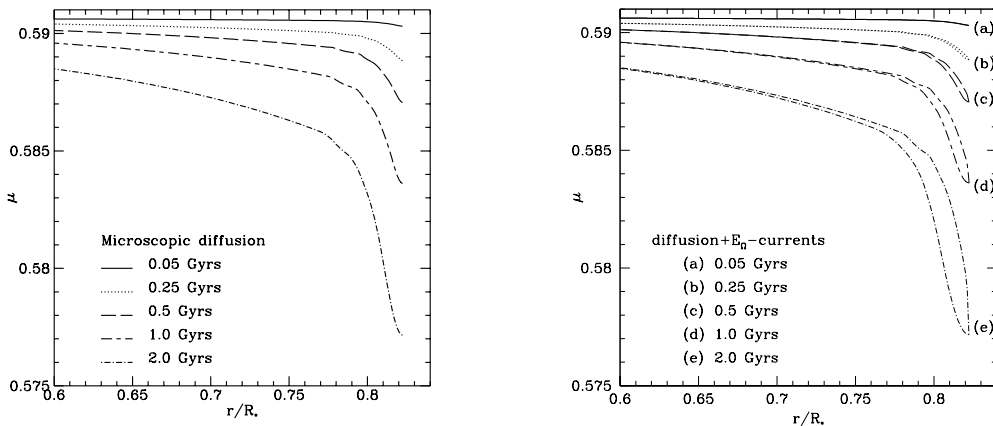


Fig. 4.— Molecular weight versus radius in each cell below the convective zone. The left figure shows the results obtained when helium microscopic diffusion is the only transport process taken into account. Under the effects of microscopic diffusion vertical  $\mu$ -gradients build below the convective zone. The horizontal microscopic diffusion is negligible so all the cells of a same shell have the same chemical composition and the same  $\mu$  value. The right figure displays the molecular weight when the diffusion of helium and the classical meridional circulation (i.e. the  $\Omega$ -currents) are introduced in the simulation. For each age two extreme curves are given. They represent at a fixed radius the spread of the  $\mu$ -values in the horizontal direction. The  $\Omega$ -currents bring  $\mu$ -enriched matter up to the rotation axis and down to the equator. This turns the vertical diffusion-induced  $\mu$ -gradients into horizontal ones which explains the spread in the value of  $\mu$  at a fixed radius.

column) compares the  $E_\Omega$  and  $E_\mu$  terms inside the stars. It shows that the horizontal  $\mu$ -gradients induced by the  $\Omega$ -currents lead rapidly to important values of  $E_\mu$ . After 0.5 Gyrs,  $E_\mu$  is already greater than  $E_\Omega$ . The described situation is then unrealistic : if such horizontal  $\mu$ -gradients were effectively built in the star, the  $\mu$ -currents should have changed the sense of the circulation. This clearly shows that the feed-back effect of  $\mu$ -currents cannot be neglected in the computations.

## 4. Meridional circulation including the $\mu$ -currents

### 4.1. The creeping paralysis

We now present the results obtained by introducing in the simulation the diffusion of helium and the two currents of meridional circulation ( $\Omega$  and  $\mu$ -currents). The advection by

the circulation is then computed by including in the computations of the meridional velocity the classical term,  $E_\Omega$  but also the  $E_\mu$  term related to the molecular weight gradients.

Figure 6 displays the  $E_\Omega$  and  $E_\mu$  profiles inside the stars at different steps of the simulation. The  $\mu$ -currents become rapidly of the same order of magnitude as the  $\Omega$ -currents below the convective zone. As soon as the two currents compensate each other, the meridional circulation seems to freeze out in the concerned regions. The frozen region first appears below the convective zone and deepens slowly inside the radiative zone. This is a “creeping paralysis” process similar to that discussed by Mestel and Moss (1986) for nuclear-induced  $\mu$ -gradients.

However the paralysis cannot be complete because of helium settling. When the horizontal  $\mu$ -gradient,  $\Lambda$ , is just equal to the critical value,  $\Lambda_{crit}$ , for which  $|E_\mu|$  is equal to  $|E_\Omega|$ , the meridional circulation vanishes. However helium diffuses out of the convection zone where it is completely homogeneous (i.e.  $\Lambda = 0$ ). Because of this diffusion, the horizontal  $\mu$ -gradients decreases below the convective zone and the circulation is triggered again until a new equilibrium state is reached. The  $E_\Omega$  and  $E_\mu$  profiles, which always remain very close in the frozen region, suggest that the balance restoring time scale below the convective zone is much more rapid than the diffusion time scale. This is the reason why this problem is difficult to treat numerically.

## 4.2. Self-regulating process

The aim of this section is to understand more accurately what happens when the balance between  $E_\Omega$  and  $E_\mu$  is broken due to the helium microscopic diffusion below the convective zone. Then, for numerical reasons, it is necessary to separate the computations of diffusion and circulation in the simulation because the balance restoring time scale is small compared to the diffusion time scale. In other words, we need to let diffusion proceed long enough to create a real unbalance, well above the numerical fluctuations, before studying the restoring effect of the circulation.

We start this study from a situation where  $|E_\Omega| = |E_\mu|$  below the convective zone in a significant region. We then stop the meridional circulation and let helium diffusion proceed further until the equilibrium between the two currents is clearly broken below the convective zone. Afterwards we stop the diffusion and introduce the circulation again in order to study its behavior.

#### 4.2.1. Computations

As an initial situation, we use the results obtained with the complete simulation after 70 Myrs (including diffusion and circulation,  $\Omega$  and  $\mu$ -currents). This situation is represented by the third graph on Figure 6 : the circulation is “paralyzed” below the convective zone down to a radius about  $r/R_* = 0.795$ . Then we stop the circulation currents, as if they were completely frozen, and we let diffusion proceed further by itself. Due to helium gravitational settling, horizontally homogeneous matter falls from the convective zone into the radiative zone. We present here the results obtained if we let the diffusion proceed alone during 400 Myrs. The upper panel of figure 7 shows the  $\Lambda$  profiles below the convective zone after the 400 Myrs of pure diffusion. Due to diffusion-induced homogenization, a significant decrease of the horizontal  $\mu$ -gradient may be observed below the convective zone ( $\Lambda < \Lambda_{crit}$ ) while  $\Lambda$  remains close to  $\Lambda_{crit}$  in the deeper layers down to the boundary of the “paralyzed” region.

We then compute again the circulation currents. The middle panel of figure 7 displays the  $E_\Omega$  and  $E_\mu$  profiles obtained at that time. As expected, the balance between the two currents is clearly broken below the convective zone : the fact that the horizontal  $\mu$ -gradient has been forced below the critical value induces that  $|E_\mu| < |E_\Omega|$ .

As a consequence, meridional circulation should settle again, with a radial velocity amplitude given by the usual  $U_r$  expression (equation 8).

The lower panel of figure 7 displays, as a function of the fractional radius, the radial flux of matter ( $\rho r^2 U_r$ ) induced by this circulation. According to equation 12, the slope of this profile determines the sign of the horizontal component of the meridional circulation. In the radiative interior ( $\rho r^2 U_r$ ) decreases with radius, which means that the horizontal velocity is positive, i.e. directed from the upward flow towards the downward flow as usual. On the other hand, just below the convective zone ( $\rho r^2 U_r$ ) increases up. Therefore, the horizontal circulation velocity is negative in this region, going from the downward flow towards the upward flow.

Figure 8 (upper panel) displays  $u_r$  and  $u_\theta$  below the convective zone for each cell of the meshpoint in the present situation and is compared to the case of the classical meridional circulation (lower panel). The graphs show the radial velocity  $u_r$  (left) or the latitudinal velocity  $u_\theta$  (right) as a function of the fractional radius, for all angles  $\theta$ .

Several interesting features arise. While the velocities are completely smooth in the classical case, three regions appear for both components in the present situation. In the deeper layers, the radial velocity is positive in a sectorial part of the star (the upward flow) and negative in the other part (downward flow) while the horizontal velocity is always positive. Above these layers the two velocities become very small (“frozen region”). Finally,

below the convective zone, the radial velocity becomes again positive in one part and negative in the other part, but the horizontal velocity is negative. Concerning the orders of magnitude, in the present situation the vertical velocity is somewhat reduced compared to the classical case, even at its maximum, while the magnitude of the horizontal velocity is significantly enhanced above and below the “frozen region”.

Figure 9 presents the resulting circulation streamlines in the deep interior and just below the convective zone. The left panel shows the circulation lines in a meridional sector after 70 Myrs of complete simulation (diffusion and circulation). The “frozen region” clearly appears below the convective zone. In the radiative interior, the circulation goes on in the classical direction but is compressed and annihilated at the bottom of the “frozen region”. In the right panel the region just below the convective zone is zoomed and expanded in  $\theta$ , after 400 Myrs of pure microscopic diffusion inside the “frozen region”. As expected from Figure 8, two circulation loops arise. In the radiative interior, the circulation remains as seen on the left panel while the second loop, which appears just below the convective zone, is clearly seen. The two loops are separated by a quiet zone with an extension  $r/R_* \simeq 3\%$

#### 4.2.2. Discussion

We have shown that, when the “frozen” state is altered by helium microscopic diffusion below the convective zone, the circulation starts again in order to compensate the created imbalance. A new circulation loop appears, opposite to the classical one. We find numerically a similar situation as described analytically in paper I. In this simulation, the two loops are separated by about half a pressure scale height. We must not forget however that this is not the real situation which occurs in stars as in the present case the circulation has been completely stopped during 400 Myrs.

The restoring time scale is very short compared to the diffusion one. If we let the circulation start again after 400 Myrs of pure helium settling, the region polluted by diffusion just below the convective zone is mixed up in less than 1 Myr due to the new loop. In consequence, we may deduce that as soon as diffusion begins to modify the equilibrium between the  $\Omega$  and the  $\mu$ -currents, the original situation is immediately restored. This corresponds to the situation described analytically in paper I, in which we showed that a stationary stage could take place, where the horizontal  $\mu$ -gradients should remain constant as well as the vertical ones, as they are consistently linked.

In the presented computations, we let the circulation start again after 400 Myrs of pure helium settling. Others computations have been done with different time scales. In any case

the restoring time scale is always very much smaller than the pure diffusion time, which is the main conclusion of this study.

## 5. Conclusion

After paper I, where we had discussed in an analytical approximate way the importance of diffusion-induced  $\mu$ -gradients on the meridional circulation in slowly rotating stars, we presented here a complete 2D simulation of the considered processes. We used a stellar model obtained from our stellar evolution code, that we discretized in the latitudinal direction. Then we computed simultaneously the helium diffusion below the convective zone and the advection due to meridional circulation. The influence of helium variations on the stellar structure was neglected (static model) but the feed-back effect of these variations on the meridional circulation was thoroughly introduced, in a complete way.

We confirmed that, in a somewhat short time scale compared to the main sequence lifetime, the so-called  $\mu$ -currents become of the same order of magnitude as the  $\Omega$ -currents, thereby creating a “frozen” region where the circulation does not proceed anymore.

However, when this occurs the equilibrium between the two opposite currents is permanently destabilized by the helium settling below the convective zone. Helium falling from the mixed outer regions induces a decrease of the horizontal  $\mu$ -gradients, which remain below the critical values for which the circulation is completely stopped. As a consequence, a new circulation loop develops, which mixes up into the convective zone the region polluted by diffusion.

We derive two important consequences of this study :

- the rotation-induced mixing which occurs in stellar radiative zones may be dramatically modified by  $\mu$ -gradients with the occurrence of disconnected loops of circulation,
- a new mixing process appears, directly induced and modulated by the microscopic diffusion.

The results concerning the rotation-induced mixing may have important consequences for the light elements which are easily destroyed by nuclear reactions ( Théado and Vauclair 2002, paper III). On the other hand, the influence of these processes on the abundance variations induced by diffusion is still not completely settled. A more sophisticated simulation would be helpful to derive it more precisely. However the results of the present 2D simulation are very encouraging. The diffusion-induced mixing which was analytically discussed in paper

I is confirmed. It acts as a restoring system for the element abundance variations and increase in a significant way their settling time scales. We suggest, as in paper I, that diffusion and mixing react in such a way as to keep both the horizontal and vertical  $\mu$ -gradients constant in the “frozen” region, while they proceed freely below.

## REFERENCES

- Chaboyer, B. and Zahn, J.-P., A&A 253, 173
- Charbonneau, P., 1992, A&A 259, 134-142
- Maeder, A. and Zahn, J.-P., 1998, A&A 334, 1000
- Mestel, L. and Moss, D. L., 1986, MNRAS 221, 25
- Montmerle, T. and Michaud, G., 1976, ApJS 31, 489
- Paquette, C., Pelletier, C., Fontaine, G., Michaud, G., 1986, ApJS 61, 177
- Tassoul, J.-L. and Tassoul, M., 1982, ApJS 49, 317
- Théado, S. and Vauclair, S., 2002, submitted to ApJ (paper III)
- Vauclair, S. and Théado, S., 2002, submitted to ApJ. (paper I)

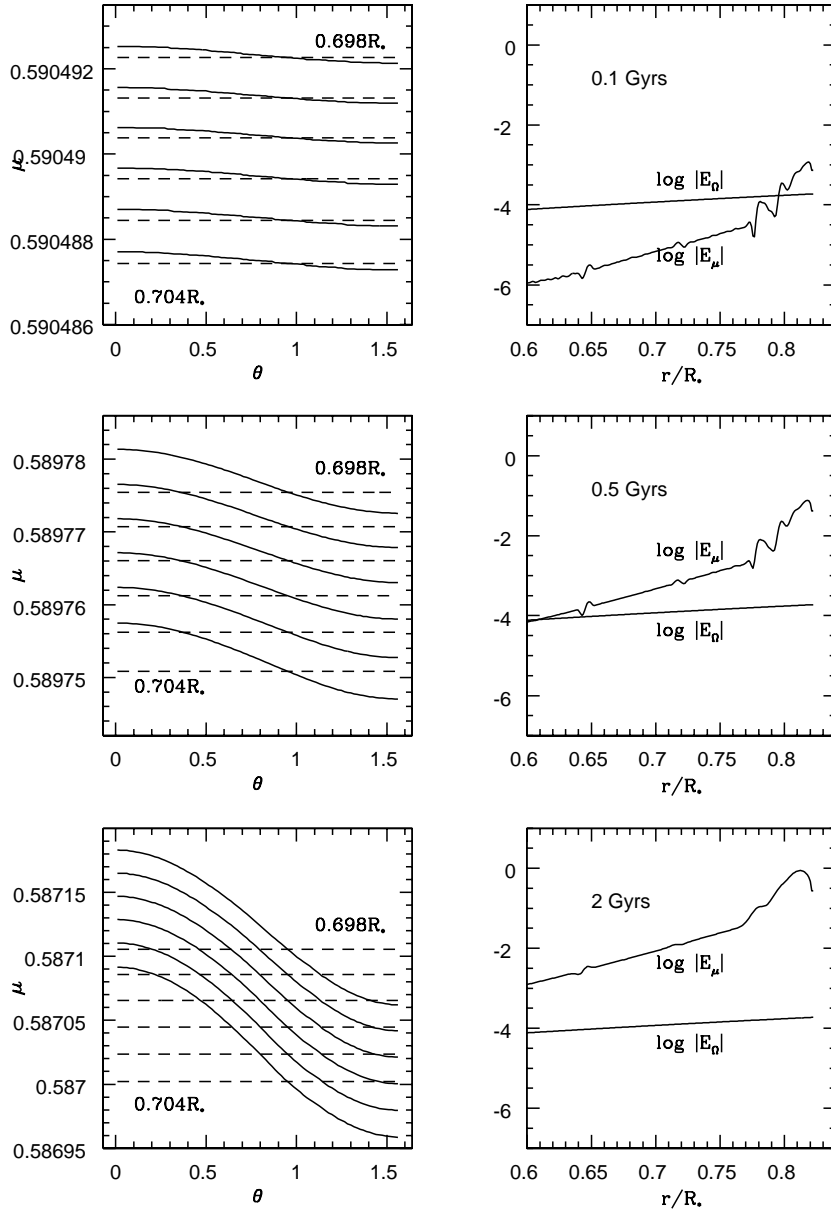


Fig. 5.— Computations including the helium microscopic diffusion and the classical meridional circulation : both the  $E_\Omega$  and the  $E_\mu$  term are computed but only the  $E_\Omega$  term is taken into account in the meridional circulation velocity computations (equation 6)). Left figure : molecular weight versus colatitude ( $\theta$  in radians) at different depth (between 0.704R<sub>\*</sub> and 0.698R<sub>\*</sub>) below the convective zone. Right :  $E_\Omega$  and  $E_\mu$  profiles inside the star. The  $E_\mu$  term, which is not introduced in the advection computations, is evaluated by computing the horizontal  $\mu$ -gradients present in the star and using the equation 8. After 0.5 Gyrs, the  $E_\mu$  term is greater than the  $E_\Omega$  term, therefore it cannot be neglected in the meridional velocity computations.

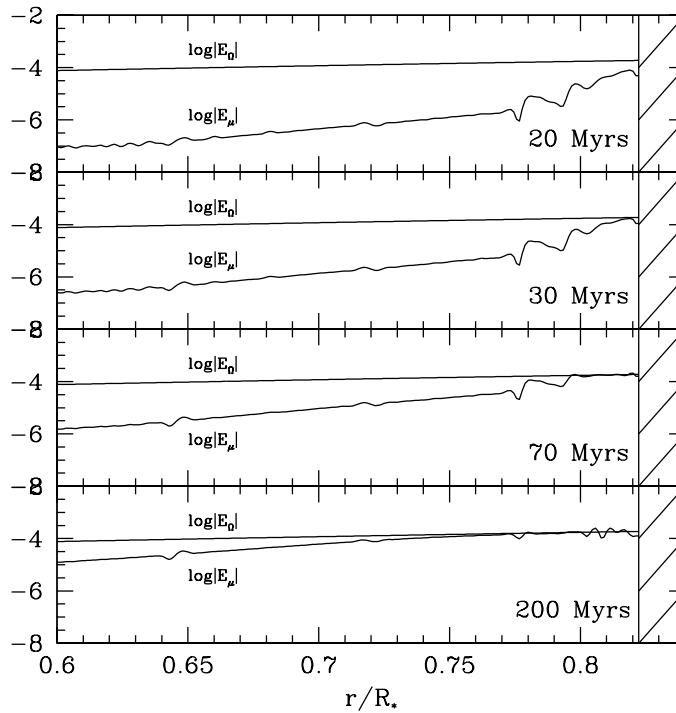


Fig. 6.— Computations including He diffusion,  $\Omega$ -currents and  $\mu$ -currents :  $E_\Omega$  and  $E_\mu$  profiles below the convective zone at different steps of the simulation. Under the combined effects of microscopic diffusion and meridional circulation, the  $\mu$ -currents increase progressively in the star. They become rapidly of the same order of magnitude as  $\Omega$ -currents below the convective zone, which freezes out the circulation in the concerned region. The paralyzed zone deepens then slowly inside the star.

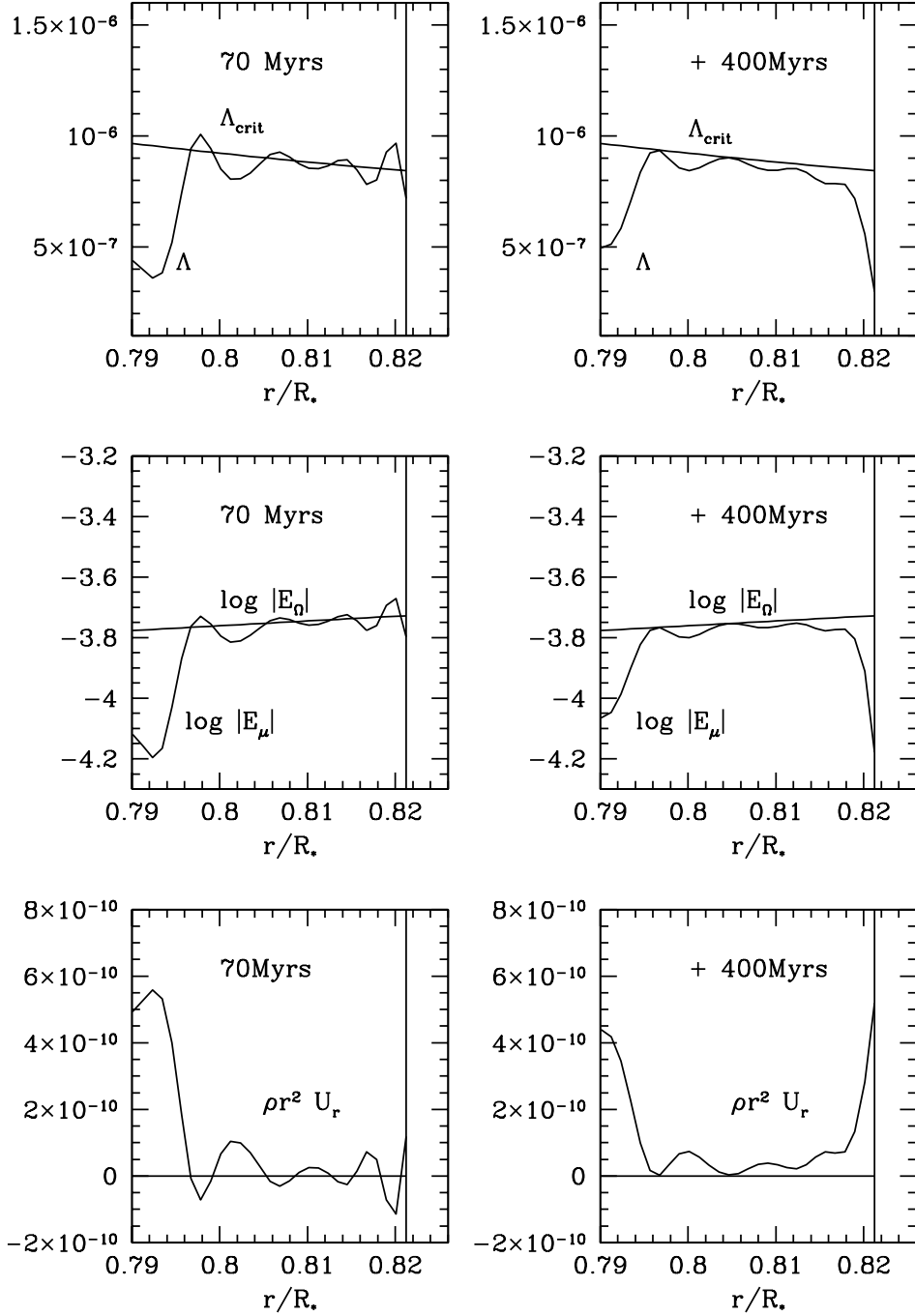


Fig. 7.— Influence of microscopic diffusion on the “creeping paralysis” below the convective zone. Left : the figures show the results obtained with the simulation (including diffusion +  $E_\Omega + E_\mu$ ) after 70 Myrs. Then we stop the circulation and let the diffusion proceed further during 400 Myrs. After this time, we stop the diffusion and introduce the circulation again. Right : the figures display the meridional circulation variables after the alteration of the equilibrium by diffusion.

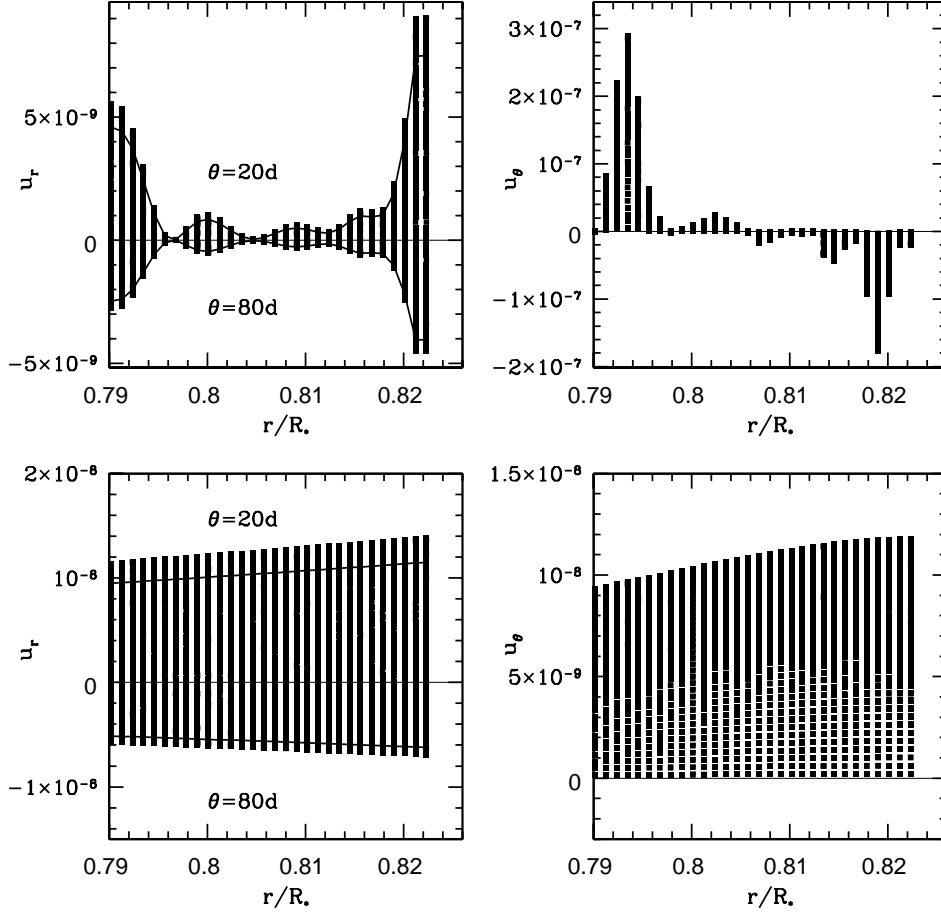


Fig. 8.— Meridional velocity components  $u_r$  (left) and  $u_\theta$  (right) below the convective zone after 400 Myrs of pure microscopic diffusion, compared to those obtained in the case of classical meridional circulation. Each cell of the meshpoint is represented by a black square, so that the velocities are shown as a function of the fractional radius, for all angles  $\theta$ . The upper and lower graphs are dramatically different. The upper graphs clearly show the effect of the “creeping paralysis” perturbed by microscopic diffusion just below the convective zone.

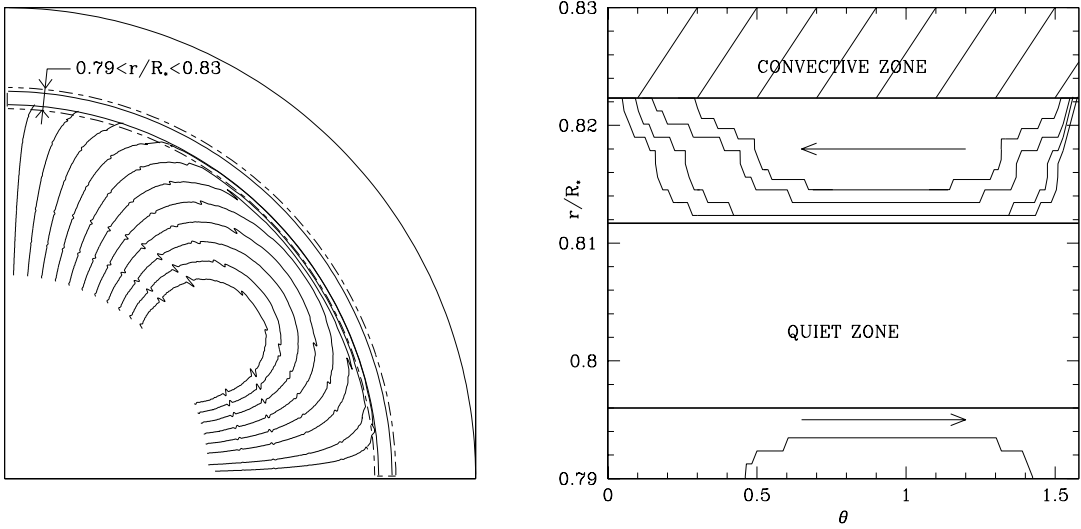


Fig. 9.— The self-regulating process. During the simulation, under the combined effects of helium diffusion and meridional circulation, the  $\mu$ -currents increase. When they become equal to  $\Omega$ -currents, the circulation vanishes. This phenomenon first occurs just below the convective zone and a frozen region appears. The left figure shows the meridional circulation streamlines obtained with the simulation after 70 Myrs. In the radiative interior, the circulation goes on in the classical direction : from the pole to the equator. Below the convective zone, the two meridional currents compensate each other and a “frozen” region has settled down in the star. Then diffusion proceeds further and homogeneous matter falls from the convective zone into the “frozen region”. It decreases the  $\mu$ -gradients and breaks up the balance between the meridional currents. The figure on the right is a zoom of the frozen region (the abscissa is  $\theta$  in radians). It shows the behavior of meridional circulation when the equilibrium between the two currents has been broken by microscopic diffusion during 400 Myrs. Two circulation loops appear. In the deep interior the meridional circulation proceeds normally, but just below the convective zone a second circulation loops settles from the equator to the pole. The two circulation loops are separated by a region where the circulation is very weak.